A Stepped Two-Phase Configuration for Switched-Reluctance Motor with High Starting Torque

A. Siadatan[1], E. Afjei[2]
1. Department of Electrical Engineering, Islamic Azad University (West Tehran Branch),
Email: a_Siadatan@sbu.ac.ir
2. Faculty of Electrical & Computer Engineering, Shahid Beheshti University G.C.,
Email: afjei@yahoo.com

Received: September 2009 Revised: November 2009 Accepted: January 2010

ABSTRACT:
The Switched Reluctance (SR) motor is a simple and robust machine, which has found application over a wide range of different power and speed shapes. This paper briefly reviews the different types of SR motors with different geometries and then presents a new configuration for a two phase SR motor with step shaped rotor poles. This motor has the ability to start and run in a specified direction without any difficulties. In other words the motor will always have starting torque no matter where the rotor is positioned. Also centrifugal switch is presented and mounted on the motor shaft for a sudden advancement of current-pulses relative to the rotor position after reaching a preset motor speed in order to develop a higher torque at starting. Then the machine is analyzed in the generator mode. To evaluate the performance of the switched reluctance machine in motoring as well as generating mode, two types of analysis, namely numerical technique and experimental study have been utilized. In the numerical analysis, due to the highly non-linear nature of the motor, a three dimensional finite element analysis is employed, whereas in the experimental study, a proto-type motor has been built and tested.

KEYWORDS: Switched Reluctance Motor, Reluctance Generator, High Starting Torque, SRM.

1. INTRODUCTION

The Development of semiconductor rectifier and power switching technology in the early 1960s led to its rapid and successful application in variable speed drives. This caused an interest in possible alternatives and simpler motor/control configurations as the switched reluctance motor. A reluctance motor consists of a rotor, which has no windings of any kind and is free to rotate between the pole pieces of a stationary singly or multiply excited magnetic structure known as the stator. Torque is produced by the tendency of the rotor to align itself with the stator magnetic field [1].

This type of motors has several advantages such as simplicity in construction, cooling, geometric versatility, durability, and higher permissible rotor temperature [2] .In general, there are four distinct types of switched-reluctance motors: namely, regular doubly salient cylindrical [3 - 4], disc-type [5 - 6], multi-layer [7], and linear motors [8]. This classification is made based upon the general shape of the motor.

The two phase switched reluctance motor has gained much attention in the past few years due to its simple motor construction as well as its drive circuit. This makes a two phase motor which uses common pole E-core structure has been introduced by Cheewoo Lee, R. Krishnan, and N. S. Lobo [10] .In this arrangement the E-core stator has three poles with the two poles at the ends having windings and the center pole has no copper windings. In [11], a new two phase switched reluctance motor utilizing a governor for the control of excitation has been presented. In [12] different geometries have been proposed whereas all of them consist of six stator poles and three rotor poles with different pole arcs and some with variable air-gaps. A detailed analysis of a 2-phase switched reluctance motor has been discussed in [13], where a significant component of the acoustic noise is suppressed or neutralized by the means of a flux-switching transition [13]. The high speed two phase switched reluctance motor with a magnetic levitated rotor is presented for high speed applications in [14]. The design aspects of two-phase switched reluctance motors for fan-applications are pointed out in [15], where it has been shown, there is reducing costs of machinery, the converter and controlling will most likely result in an oversized motor.

The Switched Reluctance Generator (SRG) is also an attractive solution for the worldwide increasing

demand of electrical energy [16]. It is inexpensive, fault tolerant with a rugged structure and operates with a high efficiency over a wide speed range. Advantages of using SRG have been proved for some applications such as the starter/generator of gas turbines in aircrafts [17, 18], windmill generators [19, 20] and as an alternator for automotive applications [1]. A new configuration for a two phase switched reluctance motor is presented in [11] which the rotor is not appropriate for mass production.

This paper presents a novel two phase configuration approach for switched reluctance motors with a high starting torque as along with experimental results obtained for the new motor with and without using a centrifugal switch for the fast advancement in firing time. This paper is organized as follows: Section II explains the motor configuration. Section III contains the numerical analysis of the prototype machine. Section IV demonstrates the Self exited generator mode. Section V presents the physical assembly of the machine as well as the experimental results obtained from the new switched reluctance machine in motoring at the generating modes which is followed by conclusions offered in section VI.

2. THE NEW CONFIGURATION

The new motor has four poles on the stator just like the regular two phase SR motor with two shaped and skewed poles on the rotor. A three dimensional view of the motor is shown in Fig. 1.

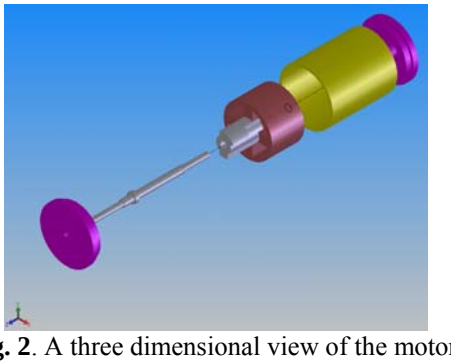

Fig. 2. A three dimensional view of the motor.

The stator geometry is the same as a regular two phase SR motor but the rotor is step-shaped in such a way to produce starting torque [21]. The shape of the rotor is shown in Fig. 2.

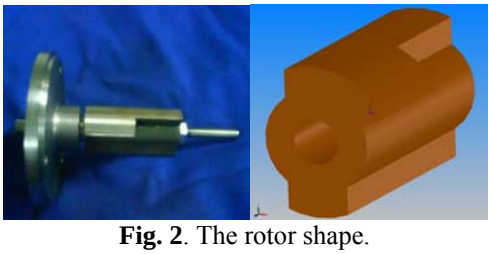

Fig. 2. The rotor shape.

The arc of rotor pole is the same as stator pole at one side but twice as big in the other side.

The design of the SRM becomes complicated due to the complex geometry and material saturation. The reluctance variation of the motor has an important role on its performance; hence an accurate knowledge of the flux distribution inside the motor for different excitation currents and rotor positions is essential for the prediction of the motor performance. The motor is highly saturated under normal operating conditions. To properly evaluate the SRM's design and performance a reliable model is required. In the presence of complex magnetic circuit geometry and nonlinear properties of the magnetic materials, the finite-element technique can be conveniently used to obtain the magnetic vector potential values throughout the motor. These vector potential values can be processed to obtain the field distribution, torque, and flux leakage.

The motor specifications considered for the study are:

stator core outer diameter	= 30mm
stator core inner diameter	= 25mm
stator arc	= 45deg.
air gap	= 0.25mm
rotor core outer diameter	= 13.5mm
rotor shaft diameter	= 4.0mm
rotor larger	= 90deg.
rotor smaller arc	= 45deg.
number of turns per pole	= 60turns

A fast acting mechanical governor is mounted on the motor shaft in order to change the dwell angle precisely for different speeds. By this way the phase commutation will begin and end sooner. This method allows for the current rise to the desired value within sufficient time. Therefore, the motoring torque will not fall off, and also, the current will be out of the winding before the rotor reaches the negative torque region.

3. NUMERICAL ANALYSIS

There are two common methods for solving magnetic field problems; one utilizes the magnetic vector potential (A), and the other one employs the electric vector potential (T). The partial differential equation for the magnetic vector potential is given by;

$$-\frac{\partial}{\partial x}\left(\gamma\frac{\partial A}{\partial x}\right)-\frac{\partial}{\partial y}\left(\gamma\frac{\partial A}{\partial y}\right)-\frac{\partial}{\partial z}\left(\gamma\frac{\partial A}{\partial z}\right)=J \qquad (1)$$

Where, A is the magnetic vector potential.

In the variational method, (Ritz) the solution to (1) is obtained by minimizing the following function

$$F(A)=\frac{1}{2}\iiint_{\Omega}[\gamma(\frac{\partial A}{\partial x})^2+\gamma(\frac{\partial A}{\partial y})^2+\gamma(\frac{\partial A}{\partial z})^2]d\Omega-\iiint_{\Omega}JAd\Omega \qquad (2)$$

Where Ω is the problem region of integration, the field analysis has been performed using a Magnet CAD package which is based on the variation energy minimization technique to calculate the electric vector potential. In this method, the electric vector potential shown as T- Ω, is define by:

$$J = \nabla \times T . \quad (3)$$

From Maxwell's equation we have;

$$\nabla \times H = J = \nabla \times T \quad (4)$$

Then

$$\nabla \times (H - T) = 0 \quad (5)$$

Since the vector (H-T) can be expressed as the gradient of a scalar i.e. we have

$$H = T - \nabla\Omega \quad (6)$$

Where what is a magnetic scalar potential. Since:

$$\nabla \times E = -\frac{\partial B}{\partial t} \quad (7)$$

Then:

$$\nabla \times E = \nabla \times \left[\left(\frac{1}{\sigma} \right) \nabla \times T \right] = \quad (8)$$

$$-\frac{\partial B}{\partial t} = -\mu_0 \mu_r \left(\frac{\partial}{\partial t} \right)(T - \nabla\Omega) = -\mu_0 \mu_r \left(\frac{\partial T}{\partial t} \right) - \nabla \left(\frac{\partial \Omega}{\partial t} \right)$$

That is finally reduced to the following scalar equations:

$$\nabla^2 T - \mu\sigma \left(\frac{\partial T}{\partial t} \right) = -\mu\sigma\nabla \left(\frac{\partial \Omega}{\partial t} \right) \quad (9)$$

$$\nabla^2 \Omega = 0 . \quad (10)$$

When a three dimensional magnetic field problem is solved by A and V, it is needed to solve all three components of A, whereas by using the T-Ω method, T can be simplified to produce a solution with only two components of T available.

The motor configuration used for the numerical simulation is shown in Figure 3.

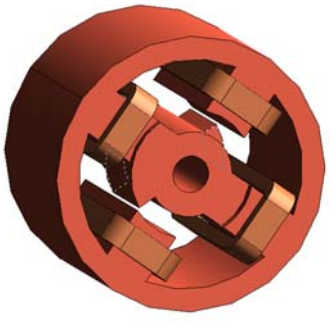

Fig. 3. The motor configuration

The 3-D field analysis has been performed using a commercial finite element package [9], which is based on the variational energy minimization technique to solve the magnetic vector potential.

The plots of magnetic flux density and its direction for the completely unaligned, beginning of alignment, half aligned, and fully aligned cases for a current magnitude of 3A are shown in figures 4, 5, 6 and 7, respectively.

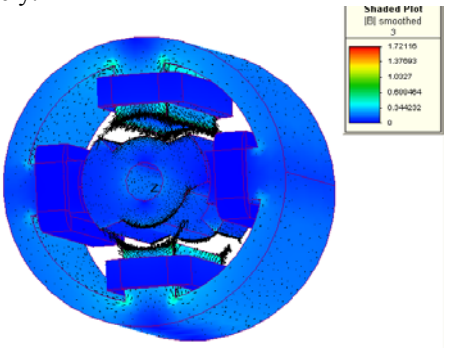

Fig. 4. magnetic flux density for the unaligned case

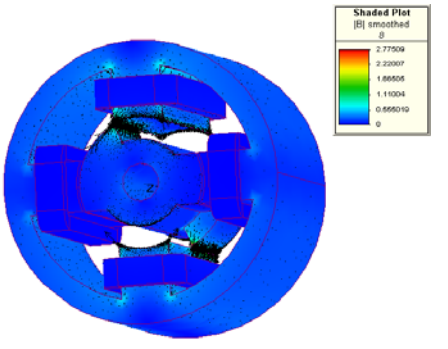

Fig. 5. magnetic flux density for the beginning of alignment

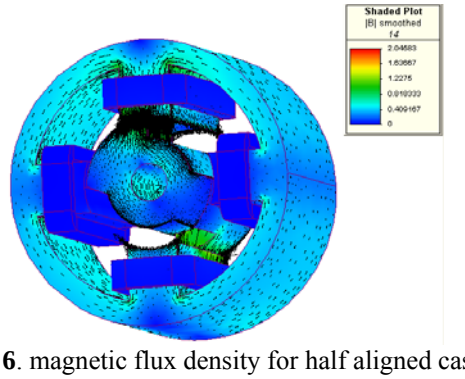

Fig. 6. magnetic flux density for half aligned case.

As it is seen in Figure 4, the stator and rotor poles are fully unaligned and the magnetic flux has a density of 1.7 Tesla on the tips of the stator poles.

Figure 5 illustrates the motor when the rotor poles are at the beginning of alignment with the stator poles. As shown in Figure 5, the aligned corners of the rotor and stator poles are in saturation and the maximum magnetic field density is about 2.8 Tesla. The direction of the magnetic flux inside the motor is also shown in

the same figure which starts from a stator pole and goes to the rotor poles and passes through the yoke to the corresponding opposite poles.

Figure 6 depicts the magnetic flux density as well as its direction for half aligned rotor and stator poles.

The maximum flux density for the aligned parts of the rotor and stator poles reaches up to about 2 Tesla as shown in Figure 6.

Finally, Figure 7 shows the rotor and stator poles in full alignment.

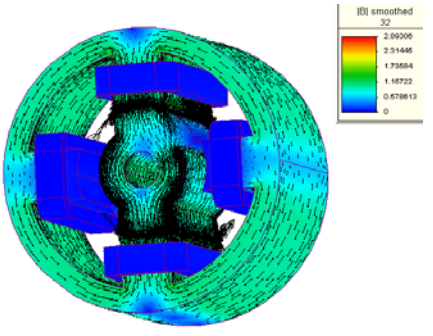

Fig. 7. Magnetic Flux Density for the Fully Aligned Case

As shown in Figure 7 the stator and rotor poles are in saturation, both with magnetic flux densities of about 2.9 Tesla.

The inductance has been defined as the ratio of each phase flux linkages to the exciting current (λ/I). Values based on this definition are presented in Figure 8 for the motor.

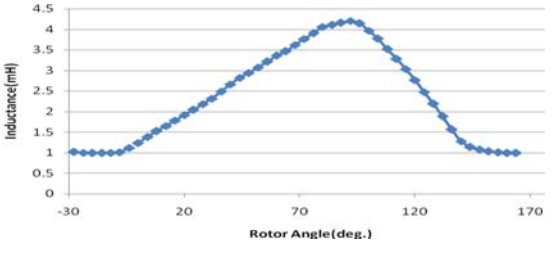

Fig. 8. Terminal inductance vs. rotor position

In the Figure 8, zero degree is considered to be at the unaligned state. The inductance profile shows a steady increase as the rotor poles move into alignment with the stator poles, hence positive torque can be obtained from 0º to 90º of the rotor arc. The inductance versus the rotor position data has been depicted by three curves; first from 0 to 45 degrees (first rotor step), second from 45 to 90 degrees (second rotor step) and finally, from 90 to 145.

Due to the step shape of the rotor which produces larger variations in flux linkage, zero to forty five degree curve shows a faster rise (higher slope) than the other one.

The plot of static torque versus rotor positions developed by the reluctance motor for a current of 3A is shown in Figure 9.

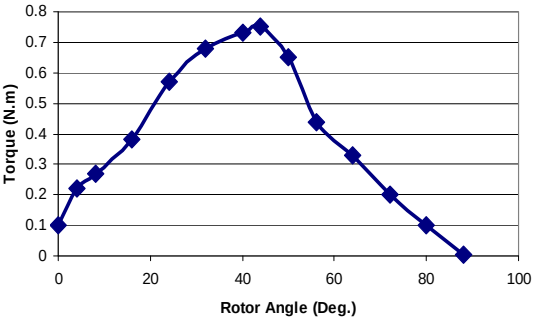

Fig. 9. Static torque versus rotor positions

The torque starts at 0.1 N.m at the beginning and reaches its maximum of about 0.75 N.m at the half alignment of stator/rotor poles and goes to zero at the full alignment. The rising and falling of static torque which is mostly due to the square of motor phase current in this type of motor curves can be estimated adequately by two second degree polynomials.

4. SELF EXCITED GENERATOR MODE

When the machine is driven by a prime mover and stator windings are excited during the negative slope of the phase inductance then the torque generating can be produced.

The torque in a SRM can be expressed lineally as

$$T = \frac{1}{2}\frac{dL}{d\theta}i^2 \qquad (11)$$

Where, L is the phase inductance, i is the motor current and θ, the rotor position.

This equation means that the torque is negative in the region of $dL/d\theta < 0$. When the stator windings are excited in that region and the rotor is driven by a proper prime mover, the mechanical energy can be transformed into electric energy. In other words, torque generation is produced when the phase winding is energized during the negative slope of the phase inductance variation, (i.e., after the complete rotor/stator poles alignment).

Due to the step shape of the rotor which produces larger variation in flux linkage, the zero to 45 degree curve shows faster rise (higher slope) than the other one from 45 to 90 degrees. The generated voltage can be obtained from the phase inductance versus rotor position by

$$e_{ind} = \frac{\partial \lambda}{\partial t} = \frac{\partial (Li)}{\partial t} = L\frac{\partial i}{\partial t} + i\frac{\partial L}{\partial t} \qquad (12)$$

Since the current, i is kept constant and $(\partial\theta/\partial t) = \omega$ then equation (4) can be rewritten as:

$$e_{ind} = i\frac{\partial L}{\partial \theta}\omega = N\frac{\partial \phi}{\partial \theta}\omega \quad (13)$$

Where, ω is motor angular speed in rad/sec.

The stator and rotor cores are made up of M-27 non-oriented silicon steel laminations. The shape of the generated voltage during negative slope of phase inductance is obtained by the inductance profile shown in figure 8 and equation 5 for a speed of 1000 rpm and shown in Figure 10.

The inductance profile is the summation of all four stator pole windings which are connected in series.

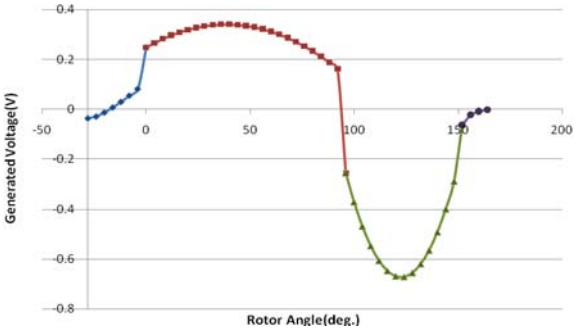

Fig. 10. Generated voltage vs. rotor position

The generated voltage shown is negative due to the negative slope of the phase inductance.

5. EXPERIMENTAL RESULTS

The motor has been fabricated and tested for its performance and functionality in the laboratory. Figure 11 illustrates the fabricated two-phase SRM.

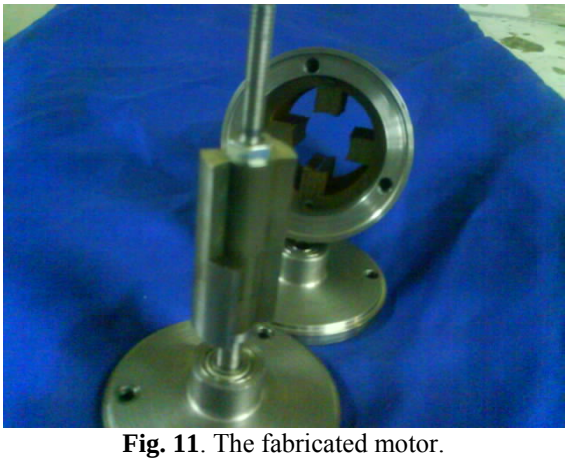

Fig. 11. The fabricated motor.

The static torque of the isolated phase was obtained by blocking the motor at different angles. The maximum static torque for a rated current of 3 A was measured to be about 0.6 N.cm. It was observed that the static torque has a lower value than the computed value which was expected, since, the silicon sheet steel material used to build the motor is actually not what is used for the numerical analysis.

The dynamic torque for the motor versus speed has been measured by loading the motor. As the motor speed increases the shape of the current waveform changes in such a way that limits the production of the motoring torque. At high speeds, it is possible for the phase current to never reach the desired value due to the self e.m.f. of the motor, therefore, the torque falls off. In order to solve this problem, the turn on phase angle is advanced in such a way that the phase commutation begins sooner. Advancing the commutation angle offers the advantages of getting the current into the phase winding while the inductance of the phase is low, and also to have a little more time to get the current out of the phase winding before the rotor reaches the negative torque region. A fast acting governor is mounted on the motor shaft in order to act as a switch. This governor opens up fast at a pre-set value of about 100 rpm, which will cause a position advancement of the rotor poles with respect to the stator poles of about 8 degrees. It is possible to use other means of changing firing time such as utilizing different set of opto-couplers or employment of some kind of a microcontroller. Using a torque meter, the dynamic torque for both motors versus their speed has been measured by loading the motors. The torque speed characteristics of the motors without employing the fast centrifugal switching action are shown in Figures 12 and 13, respectively.

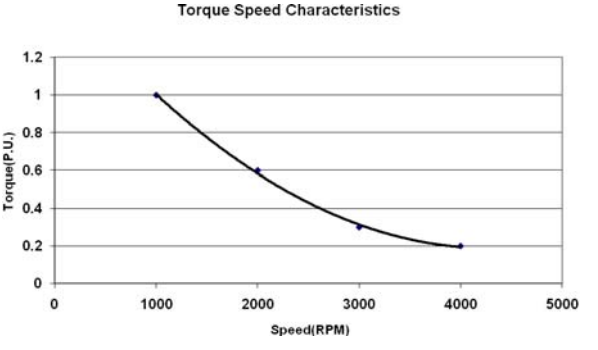

Fig. 12. Torque-speed characteristics without governor.

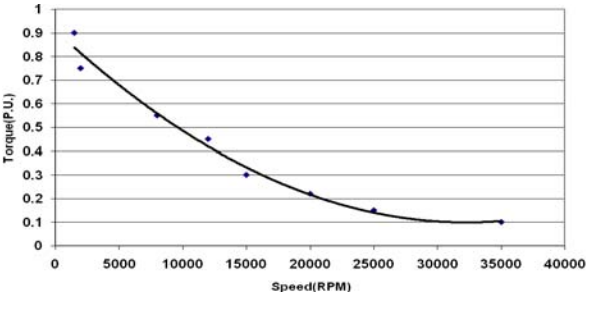

Fig. 13. Torque-speed characteristics with governor.

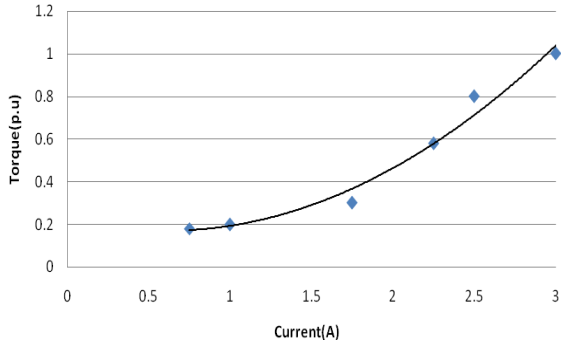

Fig. 14. Torque-current characteristics

As it is seen in Figure 13, the speed torque curve is much higher than a normal curve. The torque-speed characteristic of the motor is like a series dc motor. Figure 14 shows the torque versus the current under different loads.

The generator in the self excited mode of operation is connected to a prime mover and a two switch per phase drive circuit. The speed of rotation is set at 1000 RPM. The actual output current going in and out of the machine for one of the stator pole winding is shown in Figure 15.

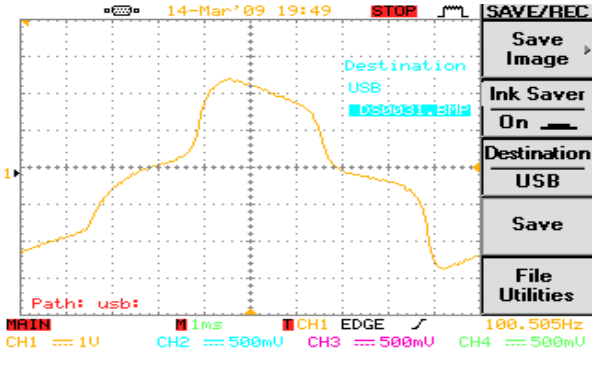

Fig. 15. The actual current for one of the stator pole winding (Self Excited)

The first part of the waveform has a positive current magnitude which means the power is entering the unit while in the other part of the waveform shows the unit in the generating mode.

There are two opto-couplers, one for each phase and a slotted disc with two 90º openings, since each rotor arc is 90º.

Figure 16 shows the output signals coming from the two photo-interrupters mounted on the back of the motor.

There are four 90o pulses produced by the motor shaft position sensors in each rotation. When one signal is at a high state the other one is at low state. Each pulse appears 2 times in one rotation for each phase since this is a two phase motor.

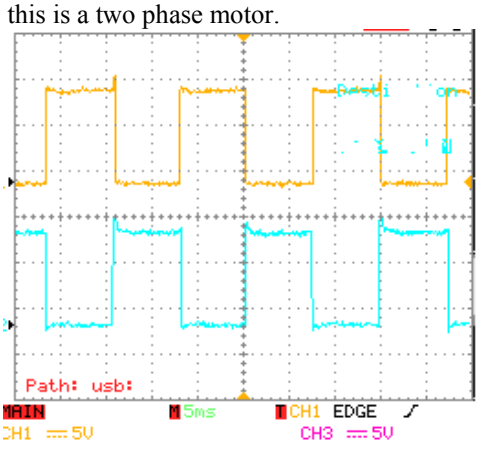

Fig. 16. The output signals from the photo-interrupters

6. CONCLUSION

In this paper a novel two phase step shaped SR motor was fabricated in the laboratory. The machine parameters in motoring as well as the generating mode were experimentally measured and tested. The two main objectives of this paper was introducing a new two phase SR motor configuration with a high starting torque, and the achievement of using centrifugal switch for fast turn-on time advancements. The experimental analysis proves the functionality of the motor in its new configuration, meaning, it has the ability and the potential of becoming a motor comparable with other types of switched reluctance motors in the industry. The fast acting switch will cause the motor to have a larger overlap area between rotor and stator poles at the beginning; hence the stating torque will be higher than a regular SR motor.

REFERENCES

[1] Fahimi B., Emad A.i and Sepe R.; **"A Switched Reluctance Machine Based Starter/Alternator for More Electric Cars"** *Energy Conversion, IEEE Transactions on Energy Conversion*, Vol. 19, Issue. 1, pp.116 – 124, (March 2004).

[2] Miller T.J.E.; **Switched Reluctance Motor Drive, Ventura, CA**, *Intertec Communications Inc*, (1988)

[3] Krishnan R.; "**Switched Reluctance Motor Drive: Modeling, Simulation, Analysis**, **Design and application"**, *Magna physics publishing*, (2001)

[4] Liang F., Liao Y. and Lipo T.A.; **"A New Variable Reluctance Motor Utilizing an Auxilary Commutation Winding**", *IEEE Tran. Ind.*, Vol. 30, No. 2, pp. 423 - 432, (March/April 1994)

[5] Bastos J.P., Goyet R., Lucidarme J., Quichaud C. and Rioux-Damidau F. **"Performance of a Multi-Disc Variable Reluctance Machine"** *International Conference on Electrical Machines, Budapest*, pp. 254 - 257, (1982)

[6] Afjei E. and Yousefi Azad; **"A Novel Disc Type Reluctance Motor"**, *International journal of*

engineering, Vol. 10, pp. 11 - 17, (Feb. 1997)

[7] Afjei E. and Toliyat H.; **"A Novel Multilayer Switched Reluctance Motor"**, *IEEE Transaction on Energy Conversion*, Vol. 17, No. 2, pp 1 – 5, (June 2002).

[8] Bae, H.K. Bae, Vijaraghavan P and Krishnan R.; **"Design of a Linear Switched Reluctance Machine"**, *IEEE Industry Appl. Conf. (IAS '99') USA*, Vol. 1, pp. 2267 -2274, (October 1999)

[9] Magnet CAD Package: User Manual, Infolytica Corporation Ltd., Montreal, Canada, (2006)

[10] Lee Cheewoo, Krishnan R. and Lobo N.S. **"New Designs of a Two-Phase E-Core Switched Reluctance Machine by Optimizing the Magnetic Structure for a Specific Application: Concept, Design, and Analysis"**, *IEEE, Industry Applications Society Annual Meeting*, pp. 1 – 8, (October 2008)

[11] Afjei E., Navi B. and Ataei S.; **"A New Two Phase Configuration for Switched Reluctance Motor with High Starting Torque"**, *IEEE, PED, Thailand*, pp. 517 - 520, (2007)

[12] Oh Seok-Gyu and Krishnan R., **"Two-Phase SRM With Flux-Reversal-Free Stator: Concept, Analysis, Design,and Experimental Verification"**, *Ieee Transactions On Industry Applications*, Vol. 43, No. 5, pp. 1247 – 1257, (September/October 2007)

[13] Pengov Wayne, Hendershot J.R. and Miller TJE, **"A New Low-Noise Two-Phase Switched Reluctance Motor"**, *IEEE International Conference Electric Machines and Drives*, pp. 1281 – 1284, (May 2005)

[14] Sun Lizhi, Yang Gang and Feng Qi; **"Study on the Rotor Levitation of one High Speed Switched Reluctance Motor"**, *IEEE Conference on Industrial Electronics*, *IECON*, pp. 1322, 1325, (November 2006)

[15] Piedler, R.W. and Doncker De; **"Designing Low-Costswitched Reluctance Drives for Fan-Applications"**, *IEEE Second International Conference on* Power Electronics, Machines and Drives, Vol. 2, pp.758 – 762, (March/April 2004)

[16] Radun A.; **"Generating with the Switched-Reluctance Motor",** *in Proc. IEEE APEC'94*, pp. 41 – 47, (1994)

[17] Mac Minn S.R. and Sember J.W., **"Control of a Switched-Reluctance Aircraft Starter-Generator Over a Very Wide Speed Range",** *in Proc. Intersociety Energy Conversion Engineering Conf*., , pp. 631 – 638, (1989)

[18] Ferreira C.A., Jones S.R, Heglund W.S. and Jones W.D.; **"Detailed Design of a 30-Kw Switched Reluctance Starter/Generator System for a Gas Turbine Engine Application"**, *IEEE Transactions on Industry Applications*, Vol. 31, Issue. 3 , (May/June 1995)

[19] Mueller M.A; **"Design of Low Speed Switched Reluctance Machines for Wind Energy Converters"**, *Electrical Machines and Drives. Ninth International Conference on* (Conf. Publ. No. 468), , pp. 60 – 64, (September 1999)

[20] Cardenas R., Ray W.F. and Asher G.M., **"Switched Reluctance Generators for Wind Energy Applications"**, *in Proc. IEEE PESC'95*, pp. 559 – 564, (1995).

[21] Afjei E.; Mazloomnezhad B. and Seyadatan A; **"A Novel Two Phase Configuration for Switched Reluctance Motor with High Starting Torque**", *in Proc. IEEE SPEEDOM* , pp. 1049 – 1052, (June 2008)